

# Design and Implementation of Uninterruptible Power Supplies for Fluorescent Lamps with Electronic Ballast

WEN-LUNG LU AND SHENG-NIAN YEH

Department of Electrical Engineering  
National Taiwan University of Science and Technology  
Taipei, Taiwan, R.O.C.

(Received October 7, 1998; Accepted April 20, 1999)

## ABSTRACT

This paper is concerned with the design and implementation of high performance uninterruptible power supplies (UPS) for fluorescent lamps with electronic ballast. The UPS design is based on the capacity and voltage ratings of the lighting equipment. The current-predicted control technique is used to control the half-bridge switch-mode rectifier so as to improve the power factor and reduce the current harmonics on the utility side. The boost/buck DC chopper is designed to charge and discharge batteries. When the utility is normal, the half-bridge switch-mode rectifier provides DC power to both the electronic ballast and the battery for the purpose of charging. This yields low current harmonic distortion and a near-unity power factor for the utility side. When the utility fails, the battery discharges quickly in order to supply DC power to the electronic ballast. A single-chip microcontroller is used to implement digitized control of the proposed system. Simulated and experimental results for a 500W prototype are presented to justify the analysis.

**Key Words:** uninterruptible power supply, half-bridge switch-mode rectifier, boost/buck, DC chopper

## I. Introduction

The conventional use of electromagnetic ballasts in fluorescent lamps usually introduces harmonics into the utility. It also leads to a poor input power factor and low efficiency and decreases the life of fluorescent lamps. To improve the power quality and the luminance of lighting, electronic ballast (Moo *et al.*, 1996; Lee *et al.*, 1990), which possesses the merits of high efficiency, a high input power factor, no flicker, low electromagnetic interference and reduced weight, will be used in the future. Emergency lighting is very important in some applications, such as in tunnels, supermarkets and office buildings. Conventional electronic ballast for fluorescent lamps combines power factor correction circuits and harmonic restraint in one piece. This conventional design requires another uninterruptible power supply (UPS) for emergency lighting, which not only lowers efficiency, but also increases the cost. This paper presents the design and implementation of high power factor, high efficiency uninterruptible power supplies for fluorescent lamps with electronic ballast. It combines the functions of power factor correction, harmonic restraint, energy storage and efficiency improvement to supply DC power for electronic ballast. Figure 1 shows a block diagram

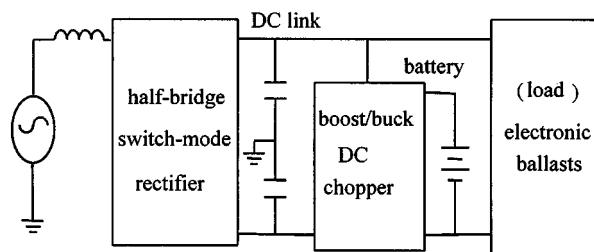


Fig. 1. Block diagram of the proposed UPS.

of the proposed UPS system. It is seen from Fig. 1 that on the utility side, a half-bridge switch-mode rectifier (Boys and Green, 1989; Hwang and Yeh, 1998; Hirachi *et al.*, 1996) is used to suppress the source harmonics current and improve the source input power factor. The boost/buck DC chopper (Rashid, 1993; Himmelstoss, 1994; Raviraj and Sen, 1997) charges and discharges the battery, keeping the DC link voltage at a fixed level. To eliminate the windup phenomenon of integral term saturation, an anti-windup proportion-integral (PI) controller (Peng *et al.*, 1996; Shin, 1998) is applied to improve performance. In addition, the current predicted control technique (Wu *et al.*, 1990; Kim *et al.*, 1994) is used to determine the switching states of the half-bridge switch-mode rectifier and boost/

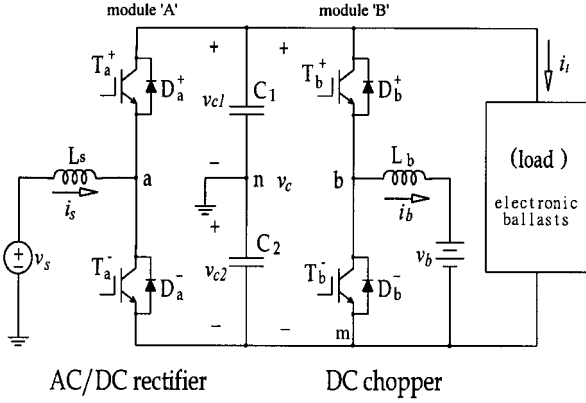


Fig. 2. UPS power circuit.

buck DC chopper. Moreover, it is worth noting that in the proposed system, a single-chip microcontroller, 80196KC, is used to implement digitized control in order to improve reliability and reduce the cost.

## II. Power Circuit

The power circuit for the proposed UPS is shown in Fig. 2. It consists of a half-bridge switch-mode rectifier, boost/buck DC chopper, inductor, capacitor and battery bank. It is seen from Fig. 2 that the proposed UPS contains two insulated-gate bipolar transistor (IGBT) modules. Module 'A' is used in the half-bridge switch-mode rectifier for AC/DC conversion while module 'B' is used in the boost/buck DC chopper for DC/DC conversion. There is only one semiconductor conduction in this topology for IGBT modules at any time, so the system can be expected to operate very efficiently (Srinivasan and Oruganti, 1997). The DC link is a cascade connection which uses two identical capacitors  $C_1$  and  $C_2$  that suppress the switching harmonics of the IGBT modules. As shown in Fig. 2, the battery absorbs energy from the DC link for the purpose of charging or releases it to supply power to the electronic ballast. Consequently, the DC link can supply power without interruption and with appropriate control. Even if a power outage occurs, the battery will discharge quickly in order to supply power and ensure continued operation.

It is seen in Fig. 2 that the same module's IGBTs cannot be turned on simultaneously. That is, when the upper-arm IGBT is on, the lower-arm IGBT must be off. Assume that the IGBT is an ideal switch in which the switching functions are  $d_1$  and  $d_2$ . When the upper-arm IGBT is on (off), the lower-arm IGBT is off (on), and the switching function is "1" ("0"). Thus, Fig. 2 can be simplified to the equivalent circuit shown in Fig. 3.

From Fig. 3, one can obtain the state equation of UPS as follows:

$$L_s \frac{d}{dt} i_s = v_s - R_s i_s - d_1 v_{c1} + (1-d_1) v_{c2}, \quad (1)$$

$$L_b \frac{d}{dt} i_b = d_2 v_{c1} + d_2 v_{c2} - R_b i_b - v_b, \quad (2)$$

$$C_1 \frac{d}{dt} v_{c1} = d_1 i_s - d_2 i_b - i_l, \quad (3)$$

$$C_2 \frac{d}{dt} v_{c2} = -(1-d_1) i_s - d_2 i_b - i_l. \quad (4)$$

From Eqs. (1)-(4), if the DC link command voltage is  $v_c^*$  and the battery command current is  $i_b^*$ , one can feed back the source current ( $i_s$ ), the DC link voltage ( $v_c$ ), the battery current ( $i_b$ ) and the battery voltage ( $v_b$ ) to design the switching functions  $d_1$  and  $d_2$  for UPS control.

In this paper, the electronic ballast contains a half-bridge series-parallel-loaded resonant (SPLR) inverter. The fluorescent lamp is modeled as a resistance for high frequency operation. Hence, the fluorescent lamp with electronic ballast can be simplified to the equivalent circuit shown in Fig. 4. (Moo *et al.*, 1996; Cosby and Nelms, 1993)

In Fig. 4,  $d_{31}$  is an ideal switch with a duty cycle of 50%. From Fig. 4, one can obtain the state equation as follows:

$$L_c \frac{d}{dt} i_{lc1} = (1-d_{31}) v_c - R_{lc} i_{lc1} - v_{c31} - v_{c41}, \quad (5)$$

$$C_3 \frac{d}{dt} v_{c31} = i_{lc1}, \quad (6)$$

$$C_4 \frac{d}{dt} v_{c41} = i_{lc1} - \frac{v_{c41}}{R_{lamp}}. \quad (7)$$

In this paper, computer simulation based on Eqs. (5)-(7) will be presented. The simulated results will be compared with those obtained from an experiment.

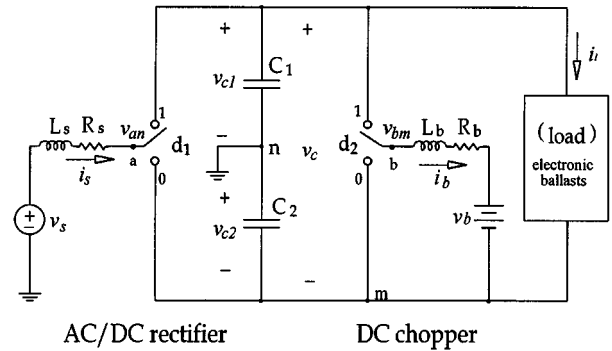


Fig. 3. UPS equivalent circuit.

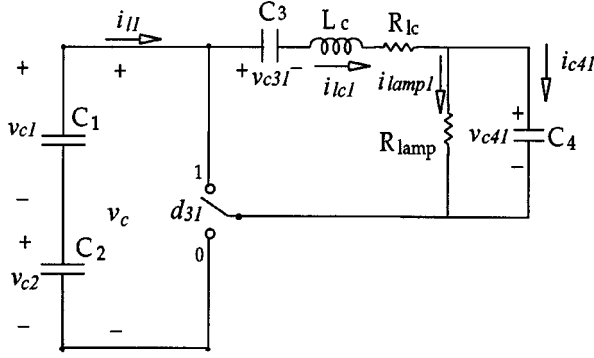


Fig. 4. Equivalent circuit of a fluorescent lamp with electronics ballast.

### III. Control of the Half-bridge Switch-mode Rectifier and Boost/Buck DC Chopper

In this paper, a current control scheme is used to control the switch-mode rectifier and the boost/buck DC chopper. Before deciding the IGBTs' switching function, the inductor current command must be calculated. For utility sides with high power factors, the source current command will be either in phase or out of phase with the source voltage. Thus, it can be represented as

$$i_s^* = I_m^* \sin \omega_e t, \quad (8)$$

where  $\omega_e$  is the source synchronous angular speed.

Hence, the peak value of the source current command  $I_m^*$  can be regulated using a proportion-integral controller to keep the DC link voltage constant. This current command will be limited for converter protection. Therefore, the system has a nonlinear region when the output of the PI controller is saturated, and system performance will deteriorate significantly due to the windup phenomenon. The windup phenomenon will result in a step response with large overshoot and long settling time. In the half-bridge circuits, the ripples component of the feedback DC link voltage is twice the source frequency and will interfere with the source current command. To improve system performance, the controller feeds back DC link voltage through a low-pass filter (LPF) to suppress the ripple components. Such a low-pass filter will degrade performance during transient response. To avoid the windup phenomenon and reduce the influence of the low-pass filter during transient response, an anti-windup PI controller is proposed. The control block diagram of  $I_m^*$  is shown in Fig. 5. When the output of the PI controller is saturated, anti-windup will be realized by a compensator that feeds back  $(I_m^* - I_{ml}^*)$  through a trans-

fer function  $F(S)$  to the integral term and switches out the low-pass filter. Normally, if the integral term is not saturated, the amplitude of the current command  $I_m^*$  can be derived as

$$I_m^* = (V_c^* - \frac{\alpha}{S + \alpha} \cdot V_c) \cdot \frac{K_{p1} \cdot (S + \beta_1)}{S} + K_{p2} \cdot I_b^*, \quad (9)$$

where

$K_{p1}, K_{p2}$ : proportional constants,

$\beta_1 \equiv K_{i1}/K_{p1}$ ,  $K_{i1}$ : the integral constant,

$\alpha$ : cut-off frequency of low-pass filter.

However, when integral-term saturation occurs, the amplitude of the current command  $I_m^*$  will become

$$I_m^* = (V_c^* - V_c) \cdot \frac{K_{p1} \cdot (S + \beta_1)}{S} - \frac{\beta_1}{S} \cdot F(S) \cdot (I_m^* - I_{ml}^*) + K_{p2} \cdot I_b^*. \quad (10)$$

Thus, anti-windup can be accomplished using the second term on the right hand side of Eq. (10).

Figure 6 is the control block diagram of the battery charging and discharging processes. When the utility is normal, the control panel produces the battery charge-

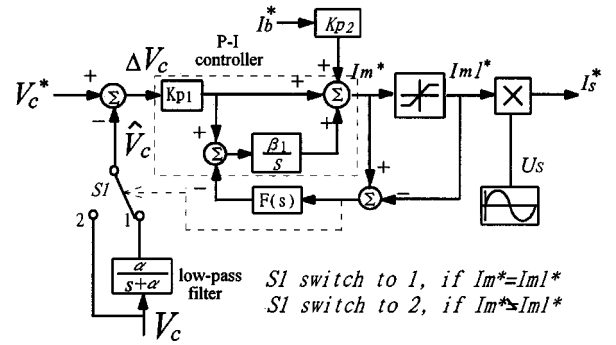


Fig. 5. The proposed control block diagram of  $I_m^*$ .

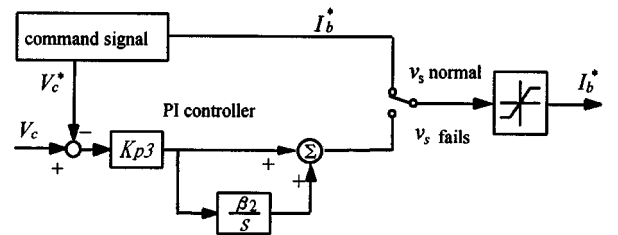


Fig. 6. Control block diagram of the battery charging and discharging processes.

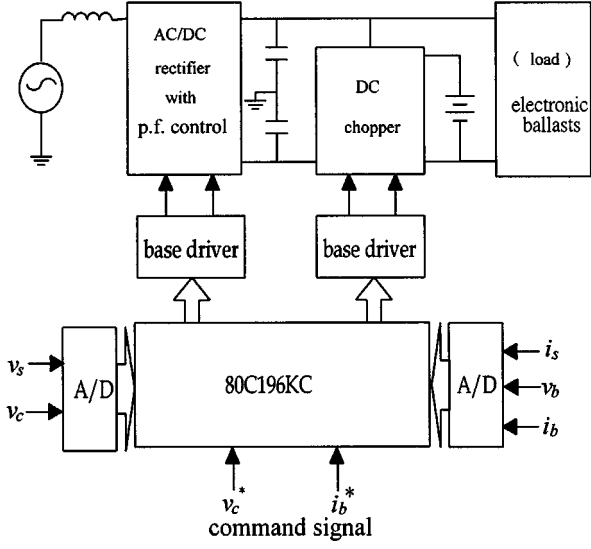


Fig. 7. The control block diagram of the proposed UPS.

ing current command  $I_b^*$  to maintain battery capacity. When the utility fails, the battery discharges quickly acts to keep the DC link voltage at voltage command  $V_c^*$ . From Fig. 6, the battery discharging command current can be expressed as

$$I_b^* = \frac{K_{p3} \cdot (S + \beta_2)}{S} \cdot (V_c - V_c^*), \quad (11)$$

where

$K_{p3}$ : the proportional constant,

$\beta_2 \equiv K_{i2}/K_{p3}$ ,  $K_{i2}$ : the integral constant.

In this paper, the current control is modeled using the current-predicted (Hwang and Yeh, 1998) control technique. The error between the current command and real current is used to compute the switching duty cycle in one period. Let  $d_1^*$  and  $d_2^*$  be the duty cycles of the switching functions  $d_1$  and  $d_2$ , respectively, and let  $T_{sw}$  be the switching period; then, from Fig. 3, the average voltages  $v_{an}^*$  and  $v_{bm}^*$  can be obtained as

$$v_{an}^* = (v_s - R_s i_s - L_s \frac{d}{dt} i_s) = d_1^* v_{c1} - (1 - d_1^*) v_{c2}, \quad (12)$$

$$v_{bm}^* = (v_b + R_b i_b + L_b \frac{d}{dt} i_b) = d_2^* v_{c1} + d_2^* v_{c2}. \quad (13)$$

Assume that

$$\frac{d}{dt} i_s = \frac{1}{T_{sw}} (i_s^* - i_s), \quad (14)$$

$$\frac{d}{dt} i_b = \frac{1}{T_{sw}} (i_b^* - i_b). \quad (15)$$

Substituting Eqs. (14) and (15) into Eqs. (12) and (13), one obtains the duty cycle commands of the IGBTs  $d_1^*$  and  $d_2^*$ :

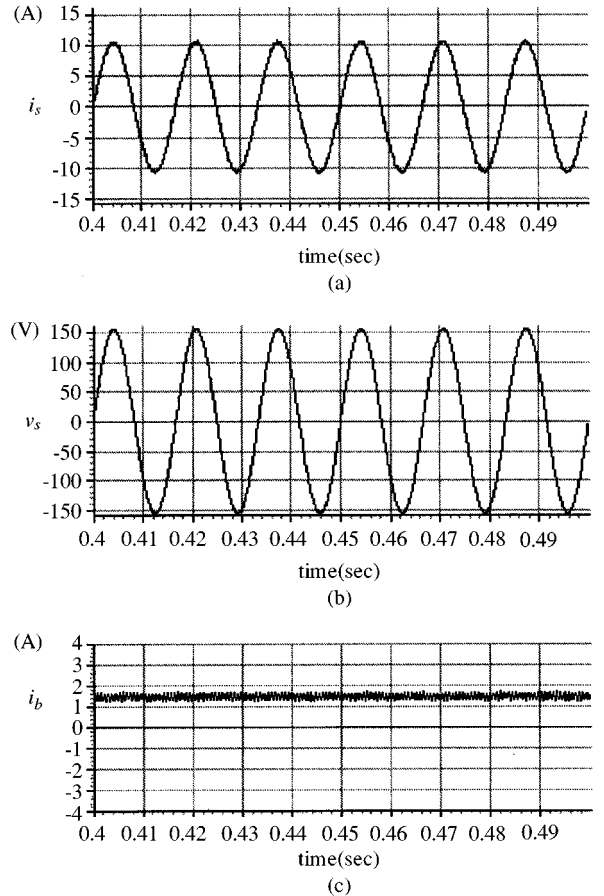
$$d_1^* = \frac{1}{v_c} [v_s - (R_s - \frac{L_s}{T_{sw}}) i_s - \frac{L_s}{T_{sw}} i_s^* + v_{c2}], \quad (16)$$

$$d_2^* = \frac{1}{v_c} [v_b + (R_b - \frac{L_b}{T_{sw}}) i_b - \frac{L_b}{T_{sw}} i_b^*]. \quad (17)$$

It can easily be seen from Eqs. (14) and (15) that if the duty cycle commands of the IGBTs are  $d_1^*$  and  $d_2^*$ , then the real current can follow the current command in one period at high switching frequency. Furthermore, in Eqs. (16) and (17), the resistances  $R_s$  and  $R_b$  can be neglected to aid realization of the circuit. The voltage  $v_{c2}$  in Eq. (16) can be replaced by  $0.5v_c$  since equal capacitors for  $C_1$  and  $C_2$  are used.

## IV. Simulation and Test Results

To verify the performance of the proposed uninter-


 Fig. 8. UPS simulated results for a load of 500 W and a battery charging current of 1.5 A: (a) source current  $i_s$ , (b) source voltage  $v_s$ , (c) battery current  $i_b$ .

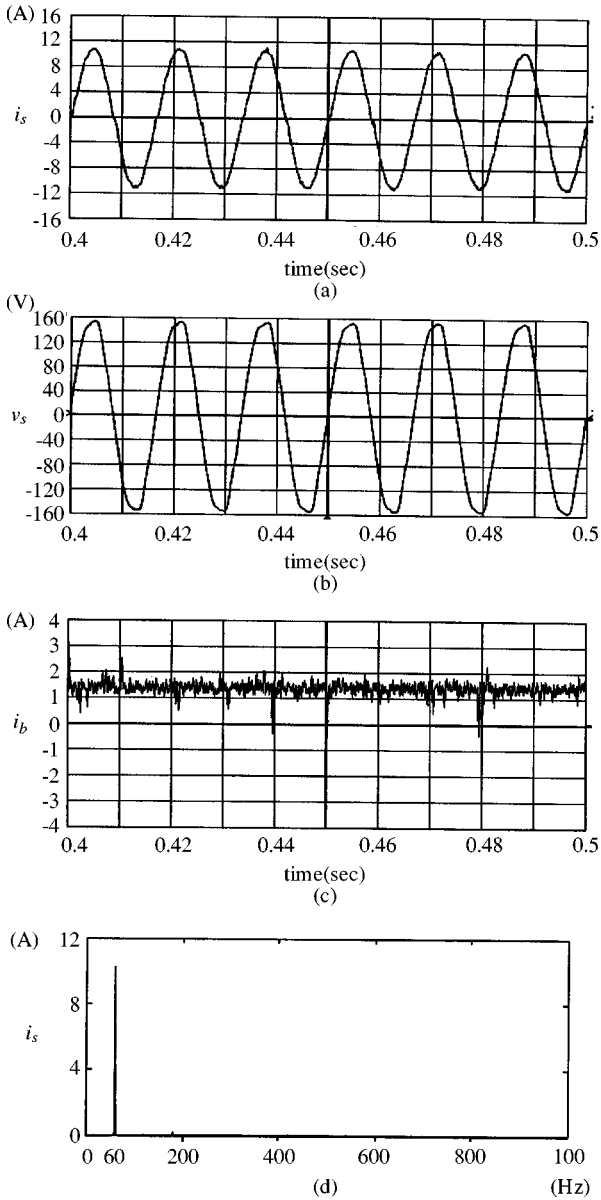


**Fig. 9.** UPS experimental results for a load of 500 W and a battery charging current of 1.5 A: (a) source current  $i_s$ , (b) source voltage  $v_s$ , (c) battery current  $i_b$ , (d) the spectrum of source current  $i_s$ .

ruptible power supplies, the complete system was simulated using SIMNON, and a 500 W prototype was developed and tested. The control block diagram of the proposed UPS is shown in Fig. 7. It consists of hardware and software in two parts. The major parameters used in the simulation and implementation of the UPS shown in Fig. 7 are as follows:

- (1) AC source voltage: 110 Vrms, 60 HZ;
- (2) battery bank: 16 batteries each with a rated voltage of 12 V and an internal resistance of 0.01  $\Omega$ ;
- (3) AC-side inductor:  $L_s=9.72$  mH (internal resis-

- tance  $R_s=0.21$   $\Omega$ );
- (4) battery side inductor:  $L_b=15.8$  mH (internal resistance  $R_b=0.32$   $\Omega$ );
- (5) DC link capacitors:  $C_1=C_2=3000$   $\mu\text{F}$ ;
- (6) digital controller switching period:  $T_s=140$   $\mu\text{S}$ ;
- (7) electronic ballast side inductor:  $L_c=4$  mH (internal resistance  $R_{1c}=4$   $\Omega$ );
- (8) electronic ballast side capacitors:  $C_3=0.1$   $\mu\text{F}$ ,  $C_4=0.01$   $\mu\text{F}$ ;
- (9) electronic ballast switching frequency: 25.5~27

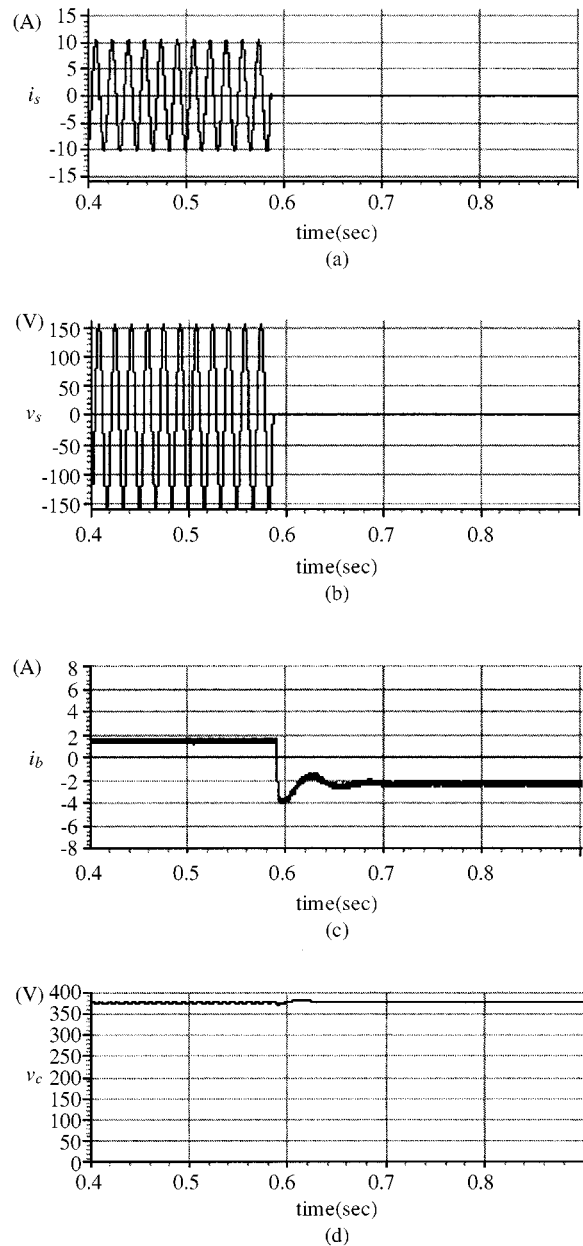


**Fig. 10.** UPS load-break simulated results for a load of 500 W and a battery charging current of 1.5 A: (a) source current  $i_s$ , (b) source voltage  $v_s$ , (c) battery current  $i_b$ , (d) DC link voltage  $v_c$ .

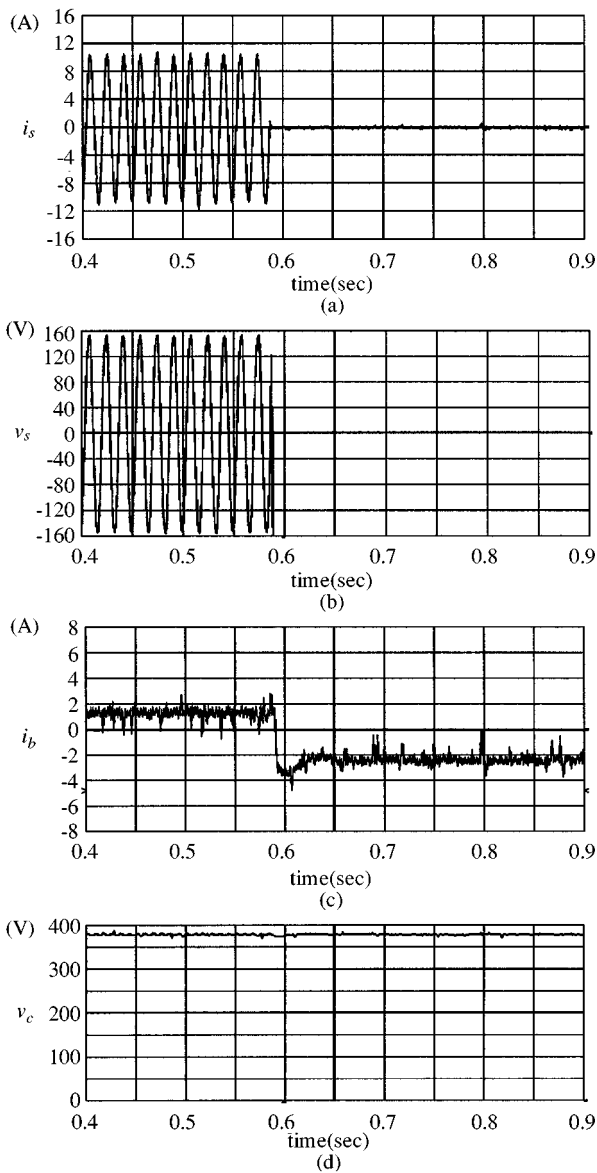


**Fig. 11.** UPS load-break experimental results for a load of 500 W and a battery charging current of 1.5 A: (a) source current  $i_s$ , (b) source voltage  $v_s$ , (c) battery current  $i_b$ , (d) DC link voltage  $v_c$ .

KHZ;

(10) fluorescent lamp steady-state equivalent resistance:  $R_{lamp}=384 \Omega$ .

Figures 8 and 9 show the simulated and experimental results obtained when the DC link voltage command  $v_c^*$  was 376 V, the load was 500 W (14 fluorescent lamps each with a rated power of 40 W), the battery charging current was 1.5 A, and the utility side total input power was 832 W. Figure 9(d) shows the spectrum of the experimental source current, the harmonic component of which was very low. Even though the total harmonic distortion of the source voltage was

3.7%, the total harmonic distortion of the source current was 4.2%. At this time, the utility side input power factor was 0.992, the DC side output power was 766.2 W and the efficiency of the half-bridge switch-mode rectifier was 92.1%. Figures 10 and 11 show the simulated and experimental results for transient response of load-break when the load was 500 W and the battery charging current was 1.5 A. It can be seen from Fig. 11(c) that the battery discharged quickly. In addition, it is obvious from Fig. 11(d) that even in the case of utility failure, the DC link voltage was almost unaffected. Figure 12 shows the transient response experimental results before and after the utility power recovered. The corresponding load was 500 W and the battery charging current was 1.5 A. Figure 13(a) and (b) show the simulated and experimental results for no-load step responses ( $v_c^*=376 \text{ V}$ ,  $v_c(0)=313 \text{ V}$ ). In Fig. 13, one can see that smaller overshoot is obtained by using an anti-windup PI controller, but that integral term saturation also occurs due to a time delay in the low pass filter. When the proposed scheme is used, however, the overshoot and settling time are reduced, and step response is improved. Figure 14(a) and (b) show the simulated and experimental results for the voltage and current of a single fluorescent lamp among all 14 lamps used. The  $v_{lamp}(\text{rms})$  was 113.3 V, the  $i_{lamp}(\text{rms})$  was 0.295 A, and the switching frequency of the electronic ballast was 26.7 KHZ. In Fig. 14(b), one can see that the voltage and current of fluorescent lamp are in phase. The fluorescent lamp becomes an

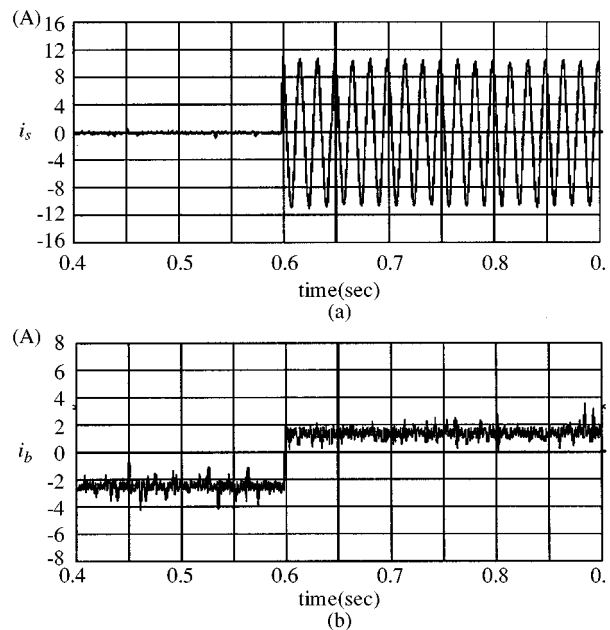


**Fig. 12.** UPS experimental results during power recovery when the load was 500 W and the battery charging current was 1.5 A: (a) source current  $i_s$ , (b) source current  $i_b$ .

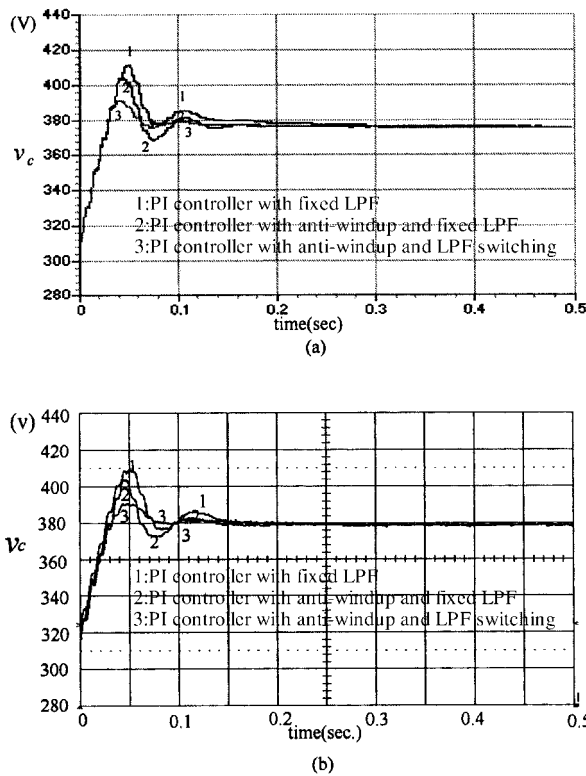


Fig. 13. The no-load step responses of the proposed UPS for  $v_c^*=376$  V,  $v_c(0)=313$ V: (a) simulated results, (b) experimental results.

equivalent resistance if operated at high switching frequency.

## V. Conclusions

In this paper, high performance uninterruptible power supplies for fluorescent lamps with electronic ballast have been explored using a half-bridge switch-mode rectifier and a boost/buck DC chopper. The validity of the proposed system configuration, which combines the functions of power factor correction, harmonics restraint, energy storage and efficiency improvement, has been verified by means of simulation and experiments. The results demonstrate that the utility side current harmonics are suppressed, and that the input power factor approaches unity. Performance evaluation results also indicate that excellent transient response is obtained under both power failure and power recovery. In addition, an anti-windup PI control scheme has been applied to overcome the windup phenomenon. The proposed 500 W prototype not only yields excellent efficiency, but also decreases costs. It could significantly improve power system quality if it were widely used.

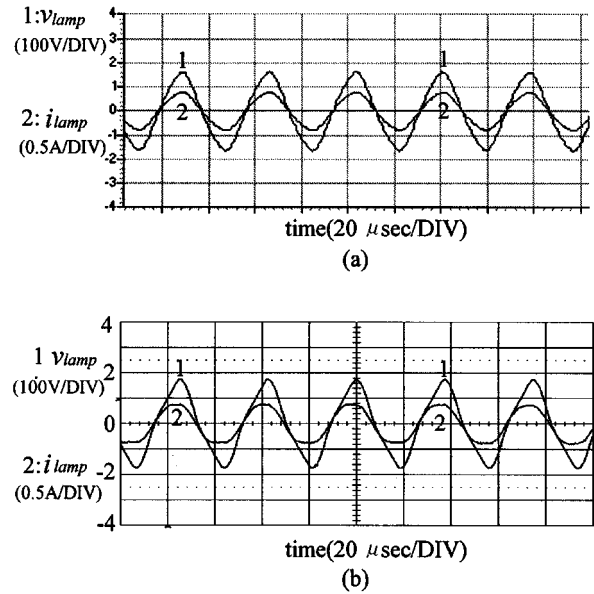


Fig. 14. The fluorescent lamp voltage  $v_{lamp}$  and current  $i_{lamp}$ : (a) simulated results, (b) experimental results.

## Acknowledgment

This work was supported by the National Science Council, R.O.C., under grant NSC 86-2213-E-011-016.

## References

- Boys, J. T. and A. W. Green (1989) Current-forced single-phase reversible rectifier. *IEE Proceedings*, **136**(5), 205-211.
- Cosby, M. C. and R. M. Nelms (1993) Design a parallel-loaded resonant inverter for an electronic ballast using the fundamental approximation. *APEC'93*, **1**, 418-423.
- Himmelstoss, F. A. (1994) Analysis and comparison of half-bridge bidirectional DC-DC converters. *IEEE PESC'94*, **2**, 922-928.
- Hirachi, K., A. Kajiyama, T. Mii, and M. Nakaoka (1996) Cost-effective bidirectional chopper-based battery link UPS with common input-output bus line and its control scheme. *IEEE IECON'96*, **3**, 1681-1686.
- Hwang, J. C. and S. N. Yeh (1998) Design and implementation of a single-phase half-bridge switch-mode rectifier. *Journal of the Chinese Institute of Electrical Engineering*, **5**(3), 213-221.
- Kim, J. M. S., P. Shanker, and W. Zhang (1994) Analysis of predictive control for active power factor correction. *IEEE IECON'94*, **1**, 446-451.
- Lee, C. H., G. B. Joung, and G. H. Cho (1990) A unity power factor high frequency parallel resonant electronic ballast. *IEEE Industry Applications Society Annual Meeting*, pp. 1149-1156. New York, NY, U.S.A.
- Moo, C. S., Y. C. Chuang, and C. R. Lee (1996) A new power factor correction circuit for electronic ballasts with series-load resonant inverter. *Proceedings of the IEEE Applied Power Electronics Conf.*, **1**, 628-633.
- Peng, Y., D. Vrancic, and R. Hanus (1996) Anti-windup, bumpless, and conditioned transfer techniques for PID controllers. *IEEE Transactions on Control Systems*, **16**, 48-57.
- Rashid, M. H. (1993) *Power Electronics Circuits, Devices and*

## Design of UPS for Fluorescent Lamps

- Applications*, pp. 303-323. Prentice Hall, Englewood Cliffs, NJ, U.S.A.
- Raviraj, V. S. C. and P. C. Sen (1997) Comparative study of proportional-integral, sliding mode, and fuzzy logic controllers for power converters. *IEEE Transactions on Industry Applications*, **33**(2), 518-524.
- Srinivasan, R. and R. Oruganti (1997) Analysis and design of power factor correction using half bridge boost topology. *IEEE APEC'97*, **1**, 489-499.
- Shin, H. B. (1998) New antiwindup PI controller for variable-speed motor drives. *IEEE Transactions on Industrial Electronics*, **45**(3), 445-450.
- Wu, R., S. Dewan, and G. Slemon (1990) A PWM AC-to-DC converter with fixed switching frequency. *IEEE Transactions on Industry Applications*, **26**(5), 880-885.

# 具電子式安定器之螢光燈不斷電系統之研製

呂文隆 葉勝年

國立台灣科技大學電機工程系

## 摘要

本文針對具電子式安定器之螢光燈電源，研製不斷電供電系統，作為緊急照明之用。依據電子式安定器所需之功率及電壓，設計適合之不斷電電源。在整流器方面，利用電流預測控制法控制半橋開關式整流器，以降低電源側電流之諧波含量及提高功率因數；在蓄電池側則藉由直流昇／降壓式截波器之控制，以調節蓄電池之充、放電能。當電源正常供電時，電能經由開關式整流器提供電子式安定器直流電源，以維持所需之照明，並將能量儲存於蓄電池中，此時電源側電流之諧波含量少，功率因數接近於1.0；當電源斷電時，蓄電池之能量經由截波器快速釋放，提供電子安定器直流電源，以維持所需之照明。本文含整體系統之設計、模擬及500 W容量之實體製作，所有控制皆由微控器(80196KC)以軟體完成，最後並以實測結果驗證此系統之性能。